New rolling horizon optimization approaches to balance short-term and long-term decisions: An application to energy planning

Étienne Cuisinier, Pierre Lemaire, Bernard Penz, Alain Ruby, Cyril Bourasseau

Version of Record: https://www.sciencedirect.com/science/article/pii/S036054422103022X
Manuscript_084f44806e86e08861277464322188be

New rolling horizon optimization approaches to balance short-term and long-term decisions : an application to energy planning

Étienne Cuisinier[a,b,*], Pierre Lemaire[b], Bernard Penz[b], Alain Ruby[a], Cyril Bourasseau[a]

[a] *CEA, LITEN, DTCH, Univ. Grenoble Alpes, Grenoble, France (17 avenue des Martyrs, 38000 Grenoble, France)*
[b] *Univ. Grenoble Alpes, CNRS, Grenoble INP, G-SCOP, 38000 Grenoble, France*

Abstract

The planning of complex systems such as energy systems calls for multiple and recurrent operational decisions depending on the present situation as well as future trends. Such decisions can be optimized with rolling-horizon approaches where most immediate decisions are fixed, based on current previsions, while next decisions are made at further optimization steps with updated information. In this paper, focus is on cases where long-term decisions have to be balanced with detailed short-term decisions to insure operational realism. On such problems, standard rolling horizon approaches are hard to solve due to the substantial increase of the temporal dimension. To overstep this issue, new approaches to balance short and long-term decisions are proposed. Two modelling approaches, based on aggregated time steps, are proposed and tested on an energy production problem where energy can be stored seasonally. Approaches are compared to benchmarks approaches (myopic and a posteriori optimization), and a sensitivity analysis is performed. Both approaches are promising and correspond to different compromises between the model complexity, computation times and solution quality.

*Corresponding author
Email addresses: etienne.cuisinier@grenoble-inp.fr (Étienne Cuisinier), pierre.lemaire@grenoble-inp.fr (Pierre Lemaire), bernard.penz@grenoble-inp.fr (Bernard Penz), alain.ruby@cea.fr (Alain Ruby), cyril.bourasseau@cea.fr (Cyril Bourasseau)

Keywords: rolling-horizon, energy planning, optimization, predictive strategy, MILP

1. Introduction

This paper proposes new rolling horizon approaches to deal with dynamic operational problems that include both short and long-term decisions. Focus is on cases where immediate short-term decisions must be modelled with a detailed discretization of time, whereas long-term decisions must be anticipated but cannot be taken in advance due to poor quality of forecast information. The new approaches are illustrated on a typical energy planning problem where energy production decisions depend on seasonal variations; however, this energy planning problem can be substituted by any production planning problem where short and long-term decisions must be balanced.

Rolling horizon (RH) approaches are common in decision making [1, 2] and are particularly relevant to solve recurrent, dynamic or multi-period problems where some immediate decisions must be made and available data can be updated through time. The idea is to solve the problem over a chosen planning horizon and using current forecasts, but to fix and effectively apply only a part of the optimized decisions. Then, for the next step, the system state as well as forecasts are updated, as in real life situations, and the problem is solved again on the shifted planning horizon. Relying on a RH can also help to divide a large optimisation problem into smaller ones. In [3], authors compare the solving of energy planning problems over the entire problem horizon with RH approaches. Finally, [4] compare LP, MILP and NLP (respectively Linear Programming, Mixed Integer Linear Programming and Non-Linear Programming) approaches, relying on a RH mechanism.

RHs are particularly applied in the energy sector. They were traditionally used to solve so-called unit commitment problems, where the set-up and the power dispatch of energy production units must be decided [5]. A RH based method is applied in [6] to optimize operations in a district heating system. In

[7], authors develop a three level RH framework for power systems and evaluates the impact of forecast accuracy. In [8], authors use a RH approach to optimize energy market bids and balancing market decisions in a stochastic framework. [9] uses a RH approach to optimize operations in an electric microgrid (i.e. electricity purchased, produced, stored, consumed and sold). In [10], [11] and [12] , authors optimize electric network operations. They rely on RH algorithms to optimize day and intra-day decisions. They investigate various models that consider the stochastic nature of the intermittent energy productions and of the demand. Authors from [13] use a RH model as a reference to evaluate several mathematical programming formulations dedicated to the design and operation optimization of an energy system. Further examples can be found in [14], [15] and [16].

In the previous examples, RHs consider short planning horizons with detailed time discretization. For instance, energy system modelling often requires an hourly discretization of time. In cases of long-term planning needs (typically when energy systems include seasonal storage), short planning horizons are limiting: a hourly planning horizon of 48 hours can fail to provide an effective use of a seasonal storage for instance. On the other hand, increasing it to 8760 hours can lead to untractable optimization problems. One could drop the RH approach and solve the problem as a single mathematical program with heuristics or decomposition techniques. However, this would require the perfect foresight assumption while the RH approaches enable to consider imperfect forecasts and information updates. Furthermore, RH approaches can include interactions of the decision model with other parties. Hence, this paper focuses on RH applications where short-term decisions should be optimized along with long-term ones. In such cases, there is a need to consider decisions over different time scales and to optimize them jointly.

This challenge was recently discussed in the energy system literature. Authors in [17] use a RH to optimize a heat supply system that includes a seasonal storage. The RH includes a few days planning horizon with seasonal storage level targets at each RH cycle. The economic objective is penalised if targets

are not met. However the penalty price is still to be found. In [18], large scale hydro-thermal systems are optimized with a RH mechanism . The long-term hydro storage is managed by introducing a value for the stored water at the end of the planning horizon. However the computation of this value is not detailed. Finally, authors from [19] simulate a microgrid with a RH. The value of storage and set-up units at the end of the planning horizon are given by a value function. The latter is estimated by solving a simplified version of the infinite horizon problem with dynamic programming.

The need for a long-term planning horizon can also occur from annual constraints or objectives like energy efficiency/savings, peak power prices, or environmental emission limits for instance. In [20], authors consider annual network charges based on an energy use threshold. They use a RH with a planning horizon based on time aggregation by representative days on the long-term. In [21], a RH is used to optimize the system operation and reach energy efficiency and energy saving targets. They rely on long-term estimations based on representative weeks. Contrarily to [20], the computations had to be done solved several times with updated estimations to reach the targets. In both cases, the continuity between aggregated periods is not kept, so such methods cannot be used if long-term decisions are path-dependent: in case a long-term storage for instance.

Finally, authors from [22] focus on the long-term degradation of batteries while optimising their daily operation in a RH model. They develop a specific parametric model to anticipate future costs of the battery deteriorating modes.

Contributions:

Few researches were found that deal with the cases where detailed short-term decisions must be optimized along with long-term decisions. This type of challenge is relevant in the field of energy research. Methods proposed in [18, 17] rely on key arbitrary values. Methods from [21] and from [20] do not keep continuity between long-term decisions. Hence they are not applicable if long-term strategies are path dependent. The method from [22] is technology specific and [19]

provides one heuristic method. Given the related problems complexity, heuristics relying on future data approximations are of interest. Different heuristics can provide different compromises between computation times, performances and simplicity. Furthermore, this can vary over the application case. Hence, authors contribute to this research gap by proposing two news approaches.

Both approaches rely on an adaptive time-step aggregation. They do not need the modeller to provide a value for long-term moves. Furthermore, both can keep the continuity between state variables over the long-term and ensure short computation times. The first one stands out for its easiness of application and short computation times with a case-dependent solution quality. The second for its potential to reach better solutions. The proposed approaches are illustrated on an energy production planning problem and can be extended to other domains.

The paper is organized as follows. The problem studied is introduced (Section 2). Then, Section 3 describes the proposed approaches. Results are shown and discussed in Section 4 and a sensitivity analysis is performed on the two best versions of the models (Section 5).

2. Problem formulation

This section presents the problem used to illustrate the proposed methodologies. It is a heat production case study: heat production units and storage must be managed to supply a network that delivers heat to dwellings corresponding to 5000 inhabitants. The time varying heat demand (D) must be supplied at each period (units considered are actually energy units). It can be supplied with two production means: an Inflexible (but cheap) Production (IFP) and a Flexible (but expensive) Production (FP). They respectively correspond to a biomass boiler and a gas boiler. Additionally, two storage units can be used: a Short-Term Storage (STS) and a Long-Term Storage (LTS). The latter has a higher capacity but lower performances.

The mathematical description of the problem is further detailed. This model

is supposed to perfectly represent the real life problem. The mathematical formulation is described on a discrete horizon $H = \{1, \ldots, \Theta \in \mathbb{N}^*\}$. The time step size (in hours) is given by dt and ensures units consistency. Variables are written in bold, continuous variables in capital letters and binary variables in small letters. In order to represent units consistency, X corresponds to units/hour and E to units. Parameters and variables are detailed below.

Production units.

- The FP unit is only defined by its unitary production cost in €/unit C^F, with no constraint on the produced quantity. Variable $\mathbf{X_t^F} \in \mathbb{R}^+$ corresponds to the production of the FP at t in units/hour.

- The IFP is characterised by a minimum and a maximum production capacity in units/hour (X^I_{min} and X^I_{max}), a maximum change of its production rate in units/hour (X^I_r), a minimum on/off time in hours (T^I_{min}), a unitary production cost in €/unit (C^I), a fixed production cost in €/hour (C^I_{on}) and a set-up cost in € (C^I_{set}). Variable $\mathbf{X_t^I} \in \{0 \cup [X^I_{min}, X^I_{max}]\}$ corresponds to the production of the IFP at t in units/hour, $\mathbf{y_t^I} \in \{0, 1\}$ equals 1 if the IFP is on at t, 0 otherwise and $\mathbf{z_t^I} \in \{0, 1\}$ equals 1 if the IFP is being set-up at t, 0 otherwise.

Storage units. Storage units (STS and LTS) are respectively defined by a maximum capacity in units (E^S_{max}, E^L_{max}), a storing efficiency (η^S, η^L) corresponding to the percentage of units that are actually stored during the storing operation (the rest is lost), losses in units lost/unit stored/hour (δ^S, δ^L) and a similar stock/destock capacity in units/hour (X^{SL}_{max}). Associated variables are the stored quantity in units ($\mathbf{E_t^S} \in [0, E^S_{max}]$ and $\mathbf{E_t^L} \in [0, E^L_{max}]$) and the stock and destock rates in units/hour ($(\mathbf{Xout_t^S}, \mathbf{Xout_t^L}, \mathbf{Xin_t^S}, \mathbf{Xin_t^L}) \in [0, X^{SL}_{max}]^4$) at time step t.

Demand. The demand (X^D_t in units/hour) has seasonal variations with higher values in winter and intermediate seasons than in summer. It also varies weakly, and daily due to external temperatures and sociological aspects.

The mathematical formulation of the problem is as follows.

Original model:

$$\min \quad \sum_{t\in H}(C^F\mathbf{X_t^F} + C^I\mathbf{X_t^I} + C^I_{on}\mathbf{y_t^I})dt + C^I_{set}\mathbf{z_t^I} \tag{E1}$$

such that

$$\forall t \in H: \quad X_t^D = \mathbf{X_t^F} + \mathbf{X_t^I} + \mathbf{Xout_t^S} + \mathbf{Xout_t^L} - \mathbf{Xin_t^S} - \mathbf{Xin_t^L} \tag{E2}$$

$$\mathbf{E_t^S} = \mathbf{E_{t-1}^S}(1-\delta^S dt) + (\eta^S\mathbf{Xin_t^S} - \mathbf{Xout_t^S})dt \tag{E3}$$

$$\mathbf{E_t^L} = \mathbf{E_{t-1}^L}(1-\delta^L dt) + (\eta^L\mathbf{Xin_t^L} - \mathbf{Xout_t^L})dt \tag{E4}$$

$$X^I_{min}\mathbf{y_t^I} \leq \mathbf{X_t^I} \tag{E5}$$

$$\mathbf{X_t^I} \leq X^I_{max}\mathbf{y_t^I} \tag{E6}$$

$$\mathbf{y_t^I} - \mathbf{y_{t-1}^I} \leq \mathbf{z_t^I} \tag{E7}$$

$$\mathbf{X_t^I} - \mathbf{X_{t-1}^I} \leq X^I_r \tag{E8}$$

$$\mathbf{X_{t-1}^I} - \mathbf{X_t^I} \leq X^I_r \tag{E9}$$

$$\forall t \in \{T^I_{min}, \ldots, \Theta\}: \quad \sum_{t'=t+1-T_{min}I}^{t} \mathbf{z_{t'}^I} \leq \mathbf{y_t^I} \tag{E10}$$

$$\forall t \in \{1, \ldots, T^I_{min}-1\}: \quad \sum_{t'=1}^{t} \mathbf{z_{t'}^I} \leq \mathbf{y_t^I} \tag{E11}$$

$$\mathbf{E_0^L} \leq \mathbf{E_\Theta^L} \tag{E12}$$

The objective $E1$ is to minimize the sum of all costs. $E2$ ensures that the demand is satisfied. $E3$ and $E4$ are the balance equations for both storage units. $E5$-$E6$ set the minimum capacity of the IFP and fixes $\mathbf{y_t^I}$. $E7$ fixes $\mathbf{z_t^I}$. $E8$-$E9$ limit the changes in the IFP production rate. The minimum on/off times of the IFP are given by $E10$-$E11$. Finally, $E12$ states that the final LTS level is at least equal to its initial level. This last constraint is only used if H corresponds to a year ($\mathbf{E_0^L}$ is set to 0 otherwise). Other variables are set to 0 if $t = 0$.

It is assumed that the problem is fully described by the above model. This problem can be solved iteratively over H in a rolling horizon fashion (see next section). However, with the possibility to store units over the long-term with the LTS, the optimal operation of the system for a given RH cycle can only be found by setting the length of H equal to a year. With an hourly time step, H would include 8760 periods which highly increases the problem dimension. To overcome this issue, new approaches are proposed in Section 3.

3. Proposed rolling horizon approaches to solve the optimization problem

This section describes the approaches proposed in this paper. They enable to solve the problem presented in Section 2 in a RH fashion by considering long-term future decisions while optimizing short-term ones.

Figure 1 describes the RH approach as well as the additional notations used in this paper. The problem is solved over a chosen planning horizon with available forecasts. Optimized decisions are effectively applied over the fixed horizon (FH). At the next cycle, H is shifted by the length of FH. The system state as well as forecasts are updated before the problem is solved again on H. This process goes infinitely.

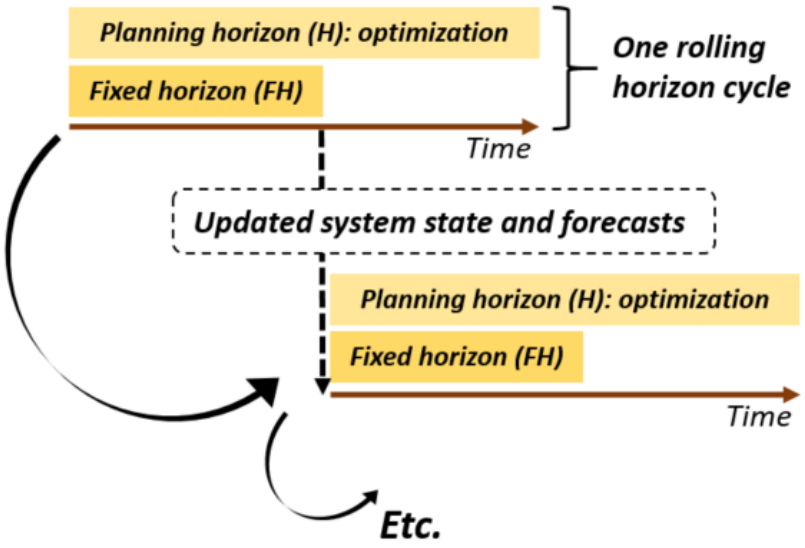

Figure 1: Rolling horizon principle

As mentioned previously, the possibility to store units over the long-term extends the planning horizon length, leading to computational issues. In order to make this extension possible, the idea of short and long-term horizons with

aggregated time steps is introduced. The horizon of the original model (H) is divided into $SH = \{1, \dots, \theta - 1\}$ and $LH = \{\theta, \dots, \Theta\}$ where $\theta \in H$ ($H = SH \cup LH$). The time step size of the original model (dt) is kept over SH while it is increased over LH. Time step aggregations were already used in other fields of energy system analysis (see [23] and [24] for instance): time steps with similar values are aggregated to reduce the problem size. Here, aggregations are made on the more distant time steps for which uncertainty increases *i.e.* the more distant, the bigger the aggregation. Hence, the time step size dt is now dependent on t: dt_t. The approach enables a long-term vision up to a year or more while limiting the total number of time steps. Furthermore, the aggregation is adapted to the immediate decision need: upcoming decisions are accurately modelled while long-term ones are reduced to necessary variables. This way, short and long-term decisions are reconciled.

The slicing (*i.e.* the values of θ and dt_t) is to be defined by the modeller. It is problem dependant. One could further define a hypothetical medium-term horizon for instance. An example of slicing is given Figure 2. This slicing naturally fits the problem of Section 2 with its actual data (see Section 4). The time step size is adapted to the forecast accuracy. Different versions of this slicing will be tested in the numerical experiments (Section 4).

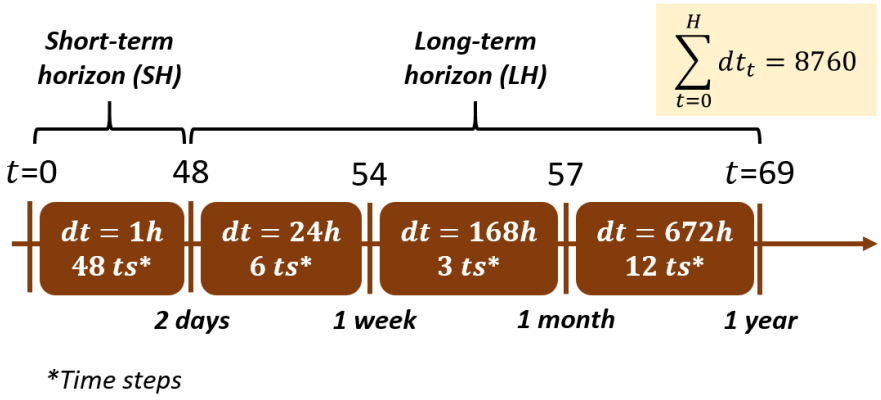

Figure 2: Planning horizon including a long-term vision with aggregated time steps

In all cases, the original MILP formulation of the problem of Section 2 is kept over SH, which includes FH. Hence, $E2$, $E5$ and $E6$ are satisfied as well as $E3$, $E4$ and $E7 - E11$ within FH. The RH mechanism ensures that $E3$, $E4$ and $E7 - E11$ are satisfied between each FH. Finally, $E12$ is satisfied because $\mathbf{E_0^L}$ is set to 0. Hence, the solution provided by the RH is a solution of $E2 - 12$.

Two models are proposed for LH to capture long-term data and decisions. The optimization is then carried out on both horizons jointly in order to keep consistency between short and long-term decisions.

3.1. Aggregation by Means and Relaxation: the M-LP model

This approach uses means of the demand over LH as an aggregation of future data. The demand $Xmean_t^D$ over the current time step t of size dt_t is the mean of the original demand over this time step. Two formulations are presented for the problem over LH.

3.1.1. Linear formulation: the original M-LP model

Here, the original MILP formulation given by $E1$-$E11$ is kept but integer variables are set to zero over LH. Variables on LH represent the means of the original continuous variables over the aggregated period. This new formulation, M-LP, is given below. Changes are marked in blue and new equations are indexed by "$EX.1$. It is assume that $T_{min}^I < \theta$.

The M-LP model is as follows:

$$\min \quad \sum_{t\in H}(C^F\mathbf{X_t^F} + C^I\mathbf{X_t^I})dt_t + \sum_{t\in SH} C^I_{on}\mathbf{y_t^I}dt_t + C^I_{set}\mathbf{z_t^I} \qquad (E1.1)$$

such that

$$\forall t \in H: \quad Xmean_t^D = \mathbf{X_t^F} + \mathbf{X_t^I} + \mathbf{Xout_t^S} + \mathbf{Xout_t^L} - \mathbf{Xin_t^S} - \mathbf{Xin_t^L} \qquad (E2.1)$$

$$\mathbf{E_t^S} = \mathbf{E_{t-1}^S}(1-\delta^S\, dt_t) + (\eta^S\mathbf{Xin_t^S} - \mathbf{Xout_t^S})\, dt_t \qquad (E3.1)$$

$$\mathbf{E_t^L} = \mathbf{E_{t-1}^L}(1-\delta^L\, dt_t) + (\eta^L\mathbf{Xin_t^L} - \mathbf{Xout_t^L})\, dt_t \qquad (E4.1)$$

$$\forall t \in SH: \quad X^I_{min}\mathbf{y_t^I} \leq \mathbf{X_t^I} \qquad (E5.1)$$

$$\mathbf{X_t^I} \leq X^I_{max}\mathbf{y_t^I} \qquad (E6.1)$$

$$\mathbf{y_t^I} - \mathbf{y_{t-1}^I} \leq \mathbf{z_t^I} \qquad (E7.1)$$

$$\mathbf{X_t^I} - \mathbf{X_{t-1}^I} \leq X^I_r \qquad (E8.1)$$

$$\mathbf{X_{t-1}^I} - \mathbf{X_t^I} \leq X^I_r \qquad (E9.1)$$

$$\forall t \in \{T^I_{min}, \ldots, \theta-1\}: \quad \sum_{t'=t+1-T_{min}I}^{t} \mathbf{z_{t'}^I} \leq \mathbf{y_t^I} \qquad (E10.1)$$

$$\forall t \in \{1, \ldots, T^I_{min}-1\}: \quad \sum_{t'=1}^{t} \mathbf{z_{t'}^I} \leq \mathbf{y_t^I} \qquad (E11)$$

$$\mathbf{E_0^L} \leq \mathbf{E_\Theta^L} \qquad (E12)$$

3.1.2. Including set-up costs: the M-LP-SetUp model

In a second formulation, set-up costs are included over LH. This is because set-up costs can be preponderant (see Section 4), thus there might be an interest in setting-up the IFP for longer than the length of SH. This is done by including the second part of $E4$, $E5$-$E7$, as well as set-up costs in the objective on LH. The model including the set-up costs is called M-LP-SetUp. Contrarily to the M-LP model, the M-LP-SetUp model is expected to better manage a potential cycling of the IFP. The MILP formulation of the M-LP-SetUp model is given below. Changes compared to the M-LP model are shown in blue and new equations are indexed by "$EX.2$".

The M-LP-SetUp model is as follows:

$$\min \quad \sum_{t\in H}((C^F\mathbf{X_t^F} + C^I\mathbf{X_t^I})dt_t + C^I_{set}\mathbf{z_t^I}) + \sum_{t\in SH} C^I_{on}\mathbf{y_t^I}dt_t \qquad (E1.2)$$

such that

$$\forall t \in H: \quad Xmean_t^D = \mathbf{X_t^F} + \mathbf{X_t^I} + \mathbf{Xout_t^S} + \mathbf{Xout_t^L} - \mathbf{Xin_t^S} - \mathbf{Xin_t^L} \qquad (E2.1)$$

$$\mathbf{E_t^S} = \mathbf{E_{t-1}^S}(1 - \delta^S dt_t) + (\eta^S\mathbf{Xin_t^S} - \mathbf{Xout_t^S})dt_t \qquad (E3.1)$$

$$\mathbf{E_t^L} = \mathbf{E_{t-1}^L}(1 - \delta^L dt_t) + (\eta^L\mathbf{Xin_t^L} - \mathbf{Xout_t^L})dt_t \qquad (E4.1)$$

$$\mathbf{X_t^I} \leq X^I_{max}\mathbf{y_t^I} \qquad (E6)$$

$$\mathbf{y_t^I} - \mathbf{y_{t-1}^I} \leq \mathbf{z_t^I} \qquad (E7)$$

$$\forall t \in SH: \quad X^I_{min}\mathbf{y_t^I} \leq \mathbf{X_t^I} \qquad (E5.1)$$

$$\mathbf{X_t^I} - \mathbf{X_{t-1}^I} \leq X^I_r \qquad (E8.1)$$

$$\mathbf{X_{t-1}^I} - \mathbf{X_t^I} \leq X^I_r \qquad (E9.1)$$

$$\forall t \in \{T^I_{min}, \ldots, \theta - 1\}: \quad \sum_{t'=t+1-T_{min}I}^{t} \mathbf{z_{t'}^I} \leq \mathbf{y_t^I} \qquad (E10.1)$$

$$\forall t \in \{1, \ldots, T^I_{min} - 1\}: \quad \sum_{t'=1}^{t} \mathbf{z_{t'}^I} \leq \mathbf{y_t^I} \qquad (E11)$$

$$\mathbf{E_0^L} \leq \mathbf{E_\Theta^L} \qquad (E12)$$

Although the M-LP-SetUp model is expected to perform better than the M-LP model, both models rely on an approximation of future costs. This approximation is based on means and on a lightened version of the original problem formulation. These models are expected to give lower bounds for the original problem over T and to underestimate future costs. In particular, the use of means leads to ignore oscillations, which are costly to the system. This justifies the elaboration of a second method described in the next section.

3.2. Aggregation by Representative Periods and Cost Functions: the RP-CF model

In order to overcome the mentioned limits of the M-LP model, the RP-CF model is introduced. It relies on an aggregation of future data by representative periods (RPs). RPs could be used directly over LH with the original MILP formulation, as performed in [20]. However, this can highly increase computation times and the continuity between time steps is lost. Hence, the RP-CF approach is proposed.

First, τ is introduced as the date corresponding to the first time step of LH. The proposed RP-CF approach relies on a pre-computation of operational costs in function of a variable which describes the long-term evolution of the system state: $c_{\tau,t}$. In our case this variable is the state of the LTS: $\Delta_t = \mathbf{E^L_t} - \mathbf{E^L_{t-1}}$. Hence, future system costs are estimated depending on the quantity moved to the LTS (possibly negative) over all periods of the LH. The functions $c_{\tau,t}$ are called the cost functions (CFs) and are defined for all periods t and for all τ.

Similarly to Section 3.1, two versions of the RP-CF model are presented: a first one without including set-up costs over LH, and a second one that includes them.

3.2.1. The original RP-CF model

Assuming that functions $c_{\tau,t}$ are known, the problem is formulated as follows. Changes to the original MILP formulation are shown in blue and new equations are indexed by "EX.3".

The RP-CF model is as follows:

min	$\sum_{t\in SH}(C^F\mathbf{X^F_t} + C^I\mathbf{X^I_t} + C^I_{on}\mathbf{y^I_t})dt_t + C^I_{set}\mathbf{z^I_t} + \sum_{t\in LH} c_{\tau,t}(\Delta_t)$	$(E1.3)$
such that		
$\forall t \in SH$:	$X^D_t = \mathbf{X^F_t} + \mathbf{X^I_t} + \mathbf{Xout^S_t} + \mathbf{Xout^L_t} - \mathbf{Xin^S_t} - \mathbf{Xin^L_t}$	$(E2.3)$
	$\mathbf{E^S_t} = \mathbf{E^S_{t-1}}(1-\delta^S\, dt_t) + (\eta^S\mathbf{Xin^S_t} - \mathbf{Xout^S_t})\, dt_t$	$(E3.3)$
	$\mathbf{E^L_t} = \mathbf{E^L_{t-1}}(1-\delta^L\, dt_t) + (\eta^L\mathbf{Xin^L_t} - \mathbf{Xout^L_t})\, dt_t$	$(E4.3)$
	$X^I_{min}\mathbf{y^I_t} \leq \mathbf{X^I_t}$	$(E5.1)$
	$\mathbf{X^I_t} \leq X^I_{max}\mathbf{y^I_t}$	$(E6.1)$
	$\mathbf{y^I_t} - \mathbf{y^I_{t-1}} \leq \mathbf{z^I_t}$	$(E7.1)$
	$\mathbf{X^I_t} - \mathbf{X^I_{t-1}} \leq X^I_r$	$(E8.1)$
	$\mathbf{X^I_{t-1}} - \mathbf{X^I_t} \leq X^I_r$	$(E9.1)$
$\forall t \in \{T^I_{min}, \ldots, \theta - 1\}$:	$\sum_{t'=t+1-T_{min}I}^{t} \mathbf{z^I_{t'}} \leq \mathbf{y^I_t}$	$(E10.1)$
$\forall t \in \{1, \ldots, T^I_{min} - 1\}$:	$\sum_{t'=1}^{t} \mathbf{z^I_{t'}} \leq \mathbf{y^I_t}$	$(E11)$
$\mathbf{E^L_0} = \mathbf{E^L_\Theta}$		$(E12)$
$\forall t \in LH$:	$\mathbf{E^L_t} = \mathbf{E^L_{t-1}}(1-\delta^L dt_t) + \Delta_t$	$(E13.3)$

Equation $E13.3$ is the storage balance equation over LH. One can note that the problem over LH is a shortest path problem.

The CFs are naturally included in the MILP formulation as piecewise linear functions. The CFs are estimated by solving the original problem over one or several RPs of the period t, for all t and for various values of Δ. The method for estimating the CFs is detailed in Appendix A for a given horizon slicing. In the case of the problem given in Section 2 and the data used in Section 4, the CFs are very close to piecewise linear functions and are convex. Slopes of the linear parts correspond to the marginal cost of the last called production unit (IFP or FP). Hence they are easily included in the MILP formulation. However, non-convex and non-linear functions would be more costly to handle.

Contrarily to the mean approximation, costs estimations based on RPs do not ignore the hourly oscillations which are costly to the system. Furthermore, costs are estimated based on the original problem formulation as opposed to the M-LP model where a linear approximation is used.

3.2.2. Side effects and inclusion of set-up costs: the RP-FC-SetUp model

Computations of CFs are subject to side effects depending on the STS and the IFP states at the beginning of the RP. In particular, set-up costs can be preponderant (see Section 4) and ignoring them over could lead to sub-optimal solutions. Hence, similarly to the M-LP-SetUp approach, the RP-FC approach is extended so that set-up costs are anticipated over the long-term. This is done by computing CFs for both assumptions:

- The IFP is already set-up at the beginning of the RP ("On" assumption).
- The IFP is off at the beginning of the RP ("Off" assumption).

Hence, two sets of CFs are obtained: c^{on} and c^{off}. This information is included in the model as follows. Changes compared to the formulation of the RP-CF model are shown in blue and new equations are indexed by "EX.4".

The RP-CF-SetUp model is as follows ($SH = \{1, \ldots, \theta-1\}$ and $LH = \{\theta, \ldots, \Theta\}$):

$$\min \quad \sum_{t \in SH} (C^F \mathbf{X_t^F} + C^I \mathbf{X_t^I} + C^I_{on} \mathbf{y_t^I}) dt_t + C^I_{set} \mathbf{z_t^I} + c^{on}_{\tau,\theta}(\Delta^{on}_\theta) + c^{off}_{\tau,\theta}(\Delta^{off}_\theta) + \sum_{t \in LH \setminus \{\theta\}} c^{on}_{\tau,t}(\Delta_t) \quad (E1.4)$$

such that

$$\forall t \in SH: \quad X^D_t = \mathbf{X_t^F} + \mathbf{X_t^I} + \mathbf{Xout_t^S} + \mathbf{Xout_t^L} - \mathbf{Xin_t^S} - \mathbf{Xin_t^L} \quad (E2.3)$$

$$\mathbf{E_t^S} = \mathbf{E^S_{t-1}}(1 - \delta^S dt_t) + (\eta^S \mathbf{Xin_t^S} - \mathbf{Xout_t^S}) dt_t \quad (E3.3)$$

$$\mathbf{E_t^L} = \mathbf{E^L_{t-1}}(1 - \delta^L dt_t) + (\eta^L \mathbf{Xin_t^L} - \mathbf{Xout_t^L}) dt_t \quad (E4.3)$$

$$X^I_{min} \mathbf{y_t^I} \leq \mathbf{X_t^I} \quad (E5.1)$$

$$\mathbf{X_t^I} \leq X^I_{max} \mathbf{y_t^I} \quad (E6.1)$$

$$\mathbf{y_t^I} - \mathbf{y^I_{t-1}} \leq \mathbf{z_t^I} \quad (E7.1)$$

$$\mathbf{X_t^I} - \mathbf{X^I_{t-1}} \leq X^I_r \quad (E8.1)$$

$$\mathbf{X^I_{t-1}} - \mathbf{X_t^I} \leq X^I_r \quad (E9.1)$$

$$\forall t \in \{T^I_{min}, \ldots, \theta - 1\}: \quad \sum_{t'=t+1-T_{min}I}^{t} \mathbf{z^I_{t'}} \leq \mathbf{y_t^I} \quad (E10.1)$$

$$\forall t \in \{1, \ldots, T^I_{min} - 1\}: \quad \sum_{t'=1}^{t} \mathbf{z^I_{t'}} \leq \mathbf{y_t^I} \quad (E11)$$

$$\mathbf{E_0^L} = \mathbf{E_\Theta^L} \quad (E12)$$

$$\forall t \in LH \setminus \{\theta\}: \quad \mathbf{E_t^L} = \mathbf{E^L_{t-1}}(1 - \delta^L dt_t) + \Delta_t \quad (E13.4)$$

$$\mathbf{E_\theta^L} = \mathbf{E^L_{\theta-1}}(1 - \delta^L dt_\theta) + \Delta^{on}_\theta + \Delta^{off}_\theta \quad (E14.4)$$

$$\Delta^{on}_\theta \leq \mathbf{y^I_{\theta-1}} E^L_{max} \quad (E15.4)$$

$$\Delta^{off}_\theta \leq (1 - \mathbf{y^I_{\theta-1}}) E^L_{max} \quad (E16.4)$$

Equation $E14.4$ is the storage balance equation exclusive to time step θ. $E15.4$-$E16.4$ ensure the consistency between the CFs c^{on} and c^{off} with the state of the IFP at $\theta - 1$.

Since the information about the state of the IFP is lost after θ, CFs computed with the "On" assumption are used afterwards ($E1.4$). This is because future costs are overestimated otherwise, which can lead to unused stored units and costly solutions. This model is called the RP-FC-SetUp model. It is expected to perform better than the RP-FC model since continuity over the IFP state is kept between SH and LH.

4. Comparison of all approaches: computational experiments

In this section, the proposed approaches are compared on the basis of the problem described in Section 2. The problem corresponds to a heat production case study: heat production units and storages must be managed to supply a network that delivers heat to 5000 inhabitants. Other production planning problems where short and long-term decisions must be balanced could be used as well. The data are shown Table 1.

Table 1: Data of the heat production problem.

Element	Parameter	Notation	Value
Flexible Production (FP), gas based	Capacity (units/hour) Cost (euros/unit)	N.A. C^F	Uncapacitated 66.8 (See Appendix D for details)
Inflexible Production (IFP), biomass based	Capacity (units/hour)	$Xmax^t$	3
	Minimum capacity (units/hour)	$Xmin^t$	1.2
	Maximum change in production (units/hour)	R^t	1.2
	Minimum up and down time (hours)	$Tmin^t$	6
	Variable cost (euros/unit)	C^t	33.3 (See Appendix D for details)
	Fixed cost (euros/hour)	Con^t	10
	Set up cost (euros)	$Cset^t$	500
Short-Term Storage (STS)	Capacity (units)	$Emax^S$	30
	Efficiency	η^S	0.98
	Losses (units/unit stored/hour)	δ^S	0.00021 (0.5% per day)
	Stock/destock capacity (units/hour)	$Xmax^S$	3
Long-Term Storage (LTS)	Capacity (units)	$Emax^L$	1500
	Efficiency (units stored/unit in)	η^L	0.97
	Losses (units/unit stored/hour)	δ^L	0.00042 (1% per day)
	Stock/destock capacity (units/hour)	$Xmax^L$	3
Demand (D)	Demand profile (units/hour)	X_t^D	See Appendix C for details

4.1. Experiments procedure

The same heat demand profile is used over both horizons SH and LH. This way, only biases on the data aggregation method and on the models themselves are accounted for. Other demand profiles as well as imperfect forecasts will be tested in Section 5.

The RH process is parametrized as follows: for all computations, the fixed horizon FH is set to 24 hours, and three different planning horizons H are tested, as defined by Figure 3. $H1$ and HM are respectively a simplified and a truncated version of $H2$.

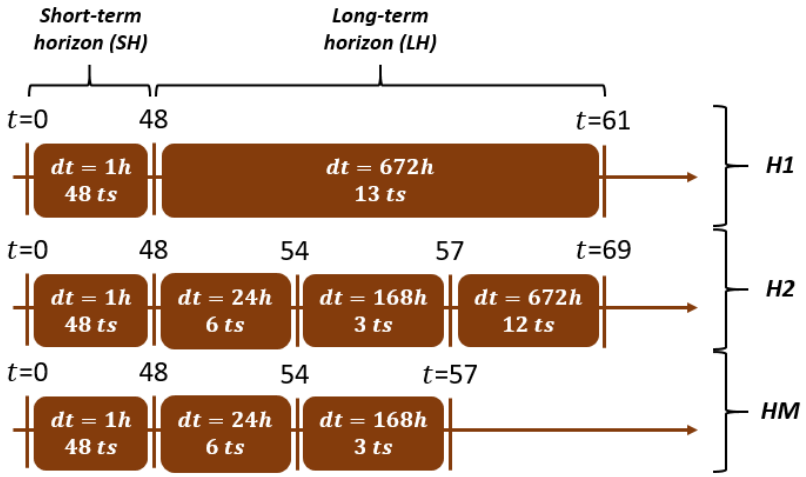

Figure 3: Planning horizons $H1$, $H2$ and HM

Two extra computations are performed to provide benchmark references:

- A *myopic approach* where the problem is solved based on a similar RH mechanism as previous approaches, except that the planning horizon H is limited to SH. This approach is used as a benchmark where forecasts are limited to 48 hours. As mentioned in Section 2, given the seasonal variations of the demand and given the possibility to store units over the

long-term with the LTS, the optimal solution might only be found by solving the problem over a year. Hence the myopic strategy suffers from the so called truncated horizon effect as defined in [25]. Storage units are emptied and the IFP is turned off at the end of H. The FH of 24 hours limits these side effects but is not sufficient to ensure an efficient long-term strategy.

- An *a posteriori optimization* of production decisions where the problem (original formulation, $E1$-$E12$) is solved over a year in a single optimization (with an hourly time discretization). This is used as a benchmark where the hourly demand is perfectly known over the whole year, which over-estimates forecast abilities and under-estimate the system operating costs. Given the problem size, only the lower and upper bounds are obtained.

All approaches are evaluated over a year. Solutions retained correspond to solutions on the Fixed Horizons FH of the RH process over a year (see Figure 4). Since the yearly strategy over the LTS might evolve if more years are simulated, models are run until it converges. In practice, this is the case after one or two years.

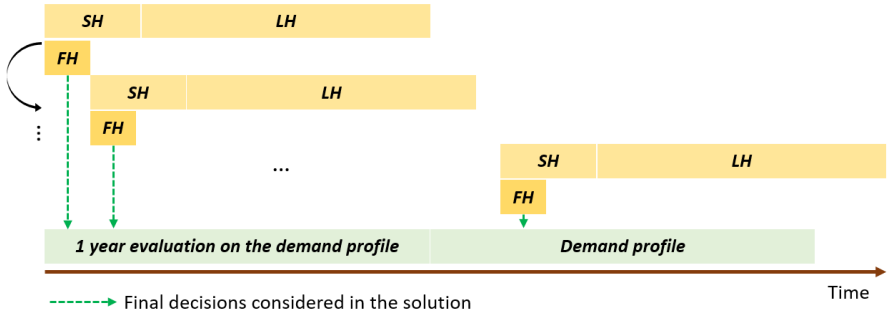

Figure 4: Evaluation process

4.2. Computational environment

Computations are performed within the PERSEE environment (see Figure 5). PERSEE is a modelling software dedicated to techno-economical assessment and design of energy systems at local, industrial and territorial scales, while optimizing their operating costs. It has been developed in CEA (Centre Energie Atomique et Energies Alternatives) since 2018 on the basis of past experiences from the Odyssey [26] and the PEGASE platforms [27]. It relies on the MILP formalism which is widely applied to deal with problems related to energy-system planning [28]. PERSEE provides a graphical user interface that allows one to model the system by assembling MILP model contributions from a C++ library, building the whole optimization problem. Multiple carriers can be used including electricity, heat or materials (gas, fuel, biomass etc.). Variables can describe energy, mass, power or mass flows. The net present value is used as the objective function. It accounts for capital and operating expenditures, replacement, purchase and sales costs as well as possible carbon emission penalties. It becomes an operating cost function when the system operation only is considered. Following up [28], PERSEE models have been written to be compliant with several time discretizations including RPs and time dependent aggregated time steps.

The problem is solved by one of the solvers available through a multi-MILP-solver interface (OSI open source, CPLEX, GUROBI etc.) As part of the PEGASE platform, PERSEE is able to control fine simulators, digital twins or real systems using model predictive control. PEGASE is compliant with the FMI-Cosimulation 2.0 norm. Both PERSEE and PEGASE are expected to be open source by 2022, in the frame of the starting CEA Trilogy project.

In this paper, the 12.9.0 version of the CPLEX solver [29] was used on an Intel Xeon Gold 6154 CPU with 2 processors of 3 GHz. The installed RAM is 96 GB. Threads used were limited to 8 threads except for the a posteriori optimization where all threads were used with a limit of 40 hours. In all cases, the final relative gap was set to 10^{-6}.

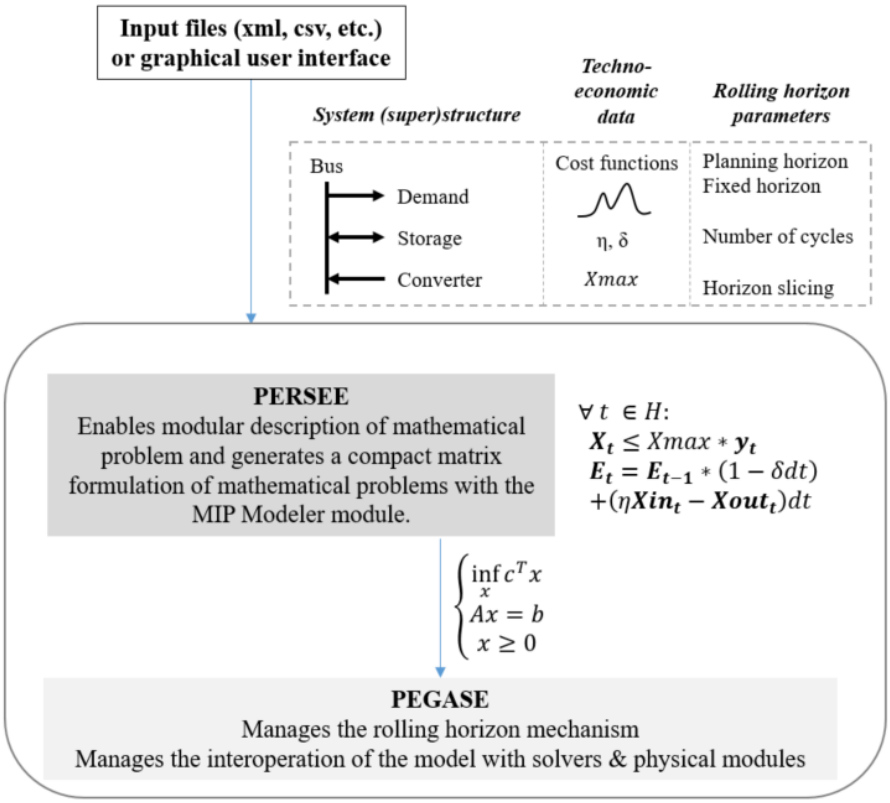

Figure 5: Schematic description of the modelling environment.

4.3. Results

4.3.1. Economic performances and computation times

Results are given in Table 2. The final relative gap with upper and lower bounds are given for the a posteriori optimization. Savings are defined as the difference between the total costs of the myopic approach with the total costs of another approach. This way, only compressible costs are considered. Savings of Table 2 are displayed on Figure 6.

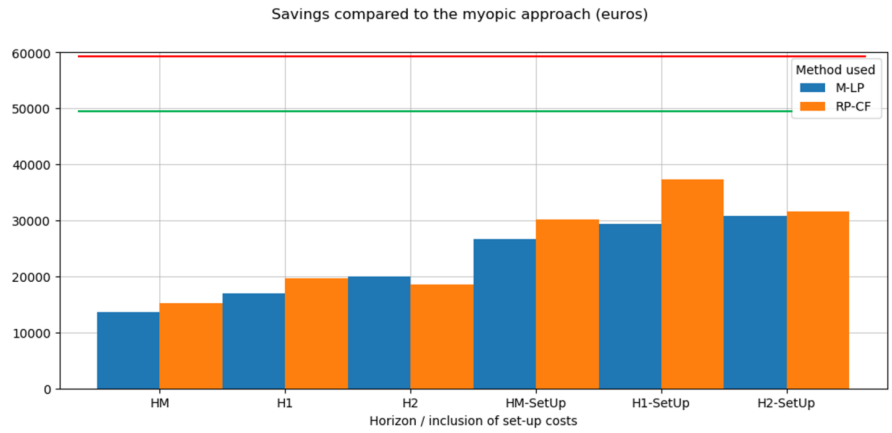

Figure 6: Savings of all approaches compared to the myopic approach (€), with upper bound (red) and lower bound (green) of the a posteriori optimization

Table 2: Results of the proposed models.

Model	Planning horizon	Total cost (euros)	Savings compared to the myopic approach (euros)	Simulation computation time (sec)	Cost functions computation time (sec)
M-LP	$H1$	847 755	16 887	36	0
M-LP-setUp	$H1$	835 340	29 302	33	0
M-LP	$H2$	844 700	19 942	33	0
M-LP-setUp	$H2$	833 924	30 718	34	0
M-LP	HM	851 083	13 559	40	0
M-LP-setUp	HM	837 918	26 724	40	0
RP-CF	$H1$	844 948	19 694	95	353
RP-CF-setUp	$H1$	827 315	37 327	95	695
RP-CF	$H2$	846 071	18 571	202	9 331
RP-CF-setUp	$H2$	833 064	31 578	253	18 641
RP-CF	HM	849 442	15 200	130	8 970
RP-CF-setUp	HM	834 456	30 186	131+131*	17 945
Myopic approach		864 642	0	32	0
A posteriori optimization		Lower bound: 806 435	58 207	40 hours Final relative gap: 1.03% RAM used: 56GB	
		Upper bound: 814 863	49 779		

*Only case where the computations converged after two years instead of one year

4.3.2. Solutions

The solutions for the benchmark myopic approach, for models M-LP, M-LP-SetUp, RP-CF, RP-CF-SetUp with horizon $H1$ and for the a posteriori optimization are described here (Figures 7 to 12). For each figure, the upper graph shows the elements of the balance equation $E2$, while the lower graph shows the state of both storages. All graphs start on the first of July.

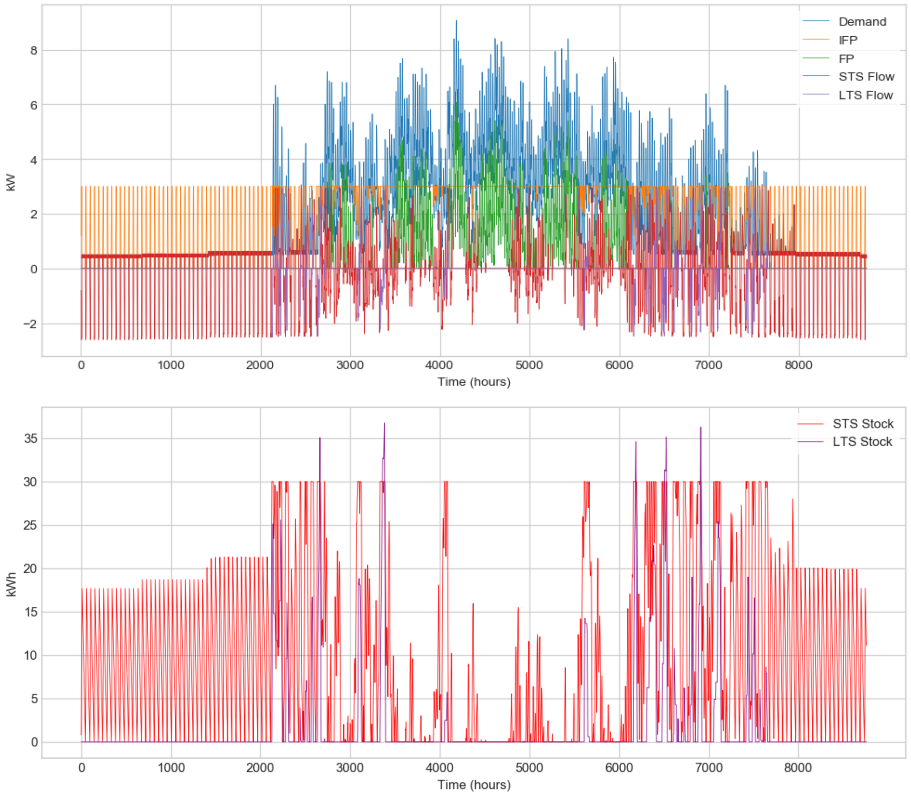

Figure 7: Results for the benchmark myopic approach.

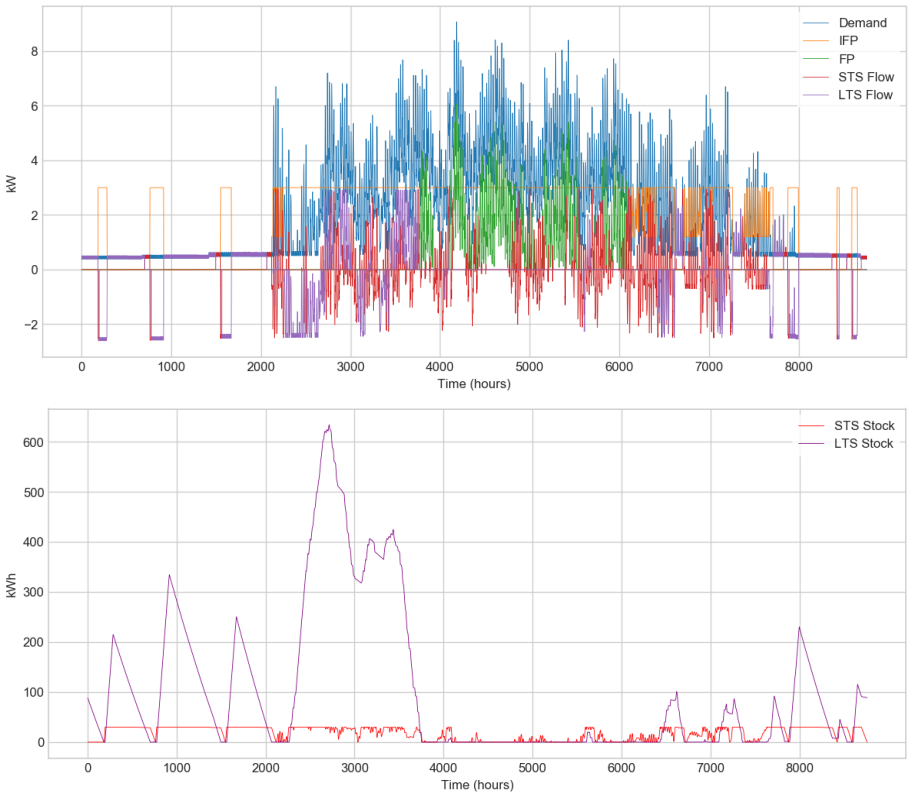

Figure 8: Results for the a posteriori optimization.

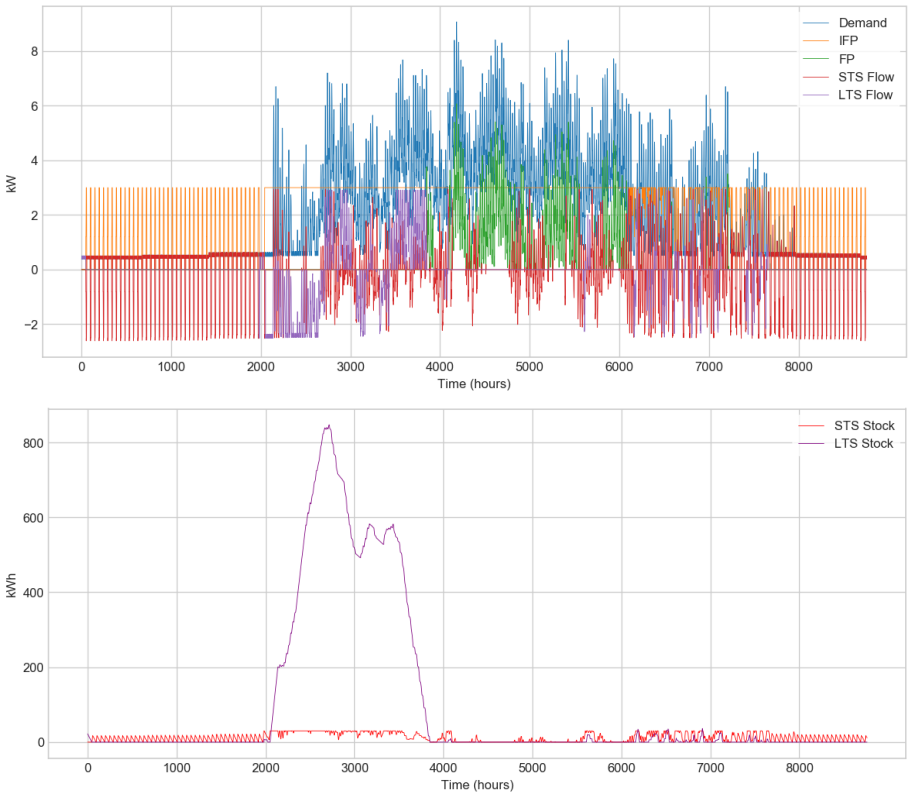

Figure 9: Results for the M-LP model.

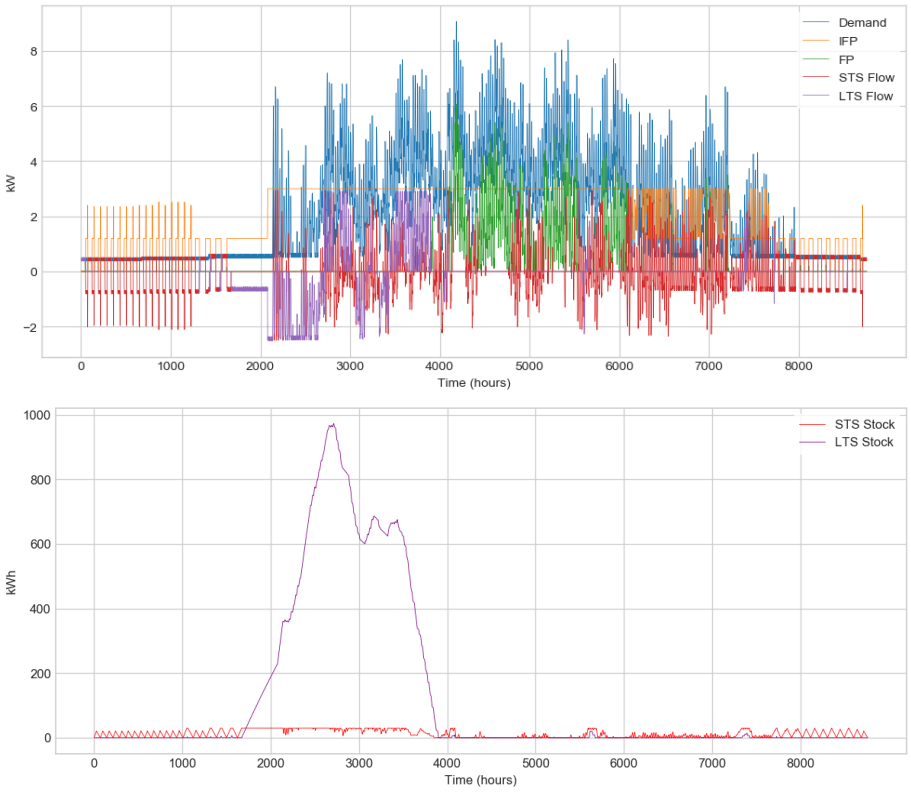

Figure 10: Results for the M-LP-SetUp model.

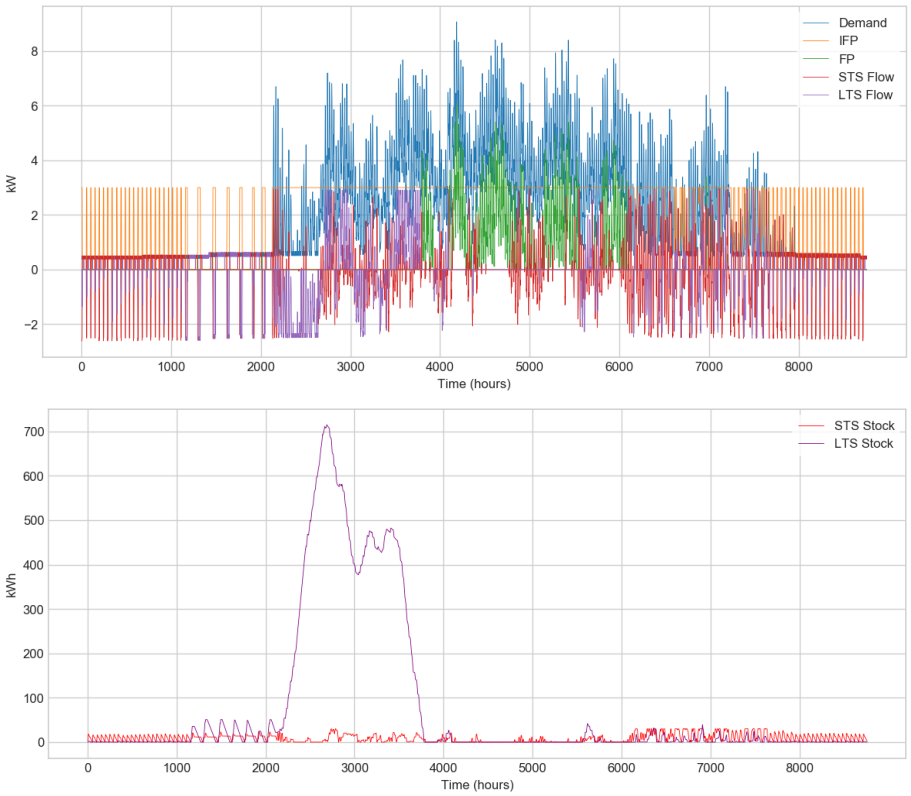

Figure 11: Results for the RP-CF model.

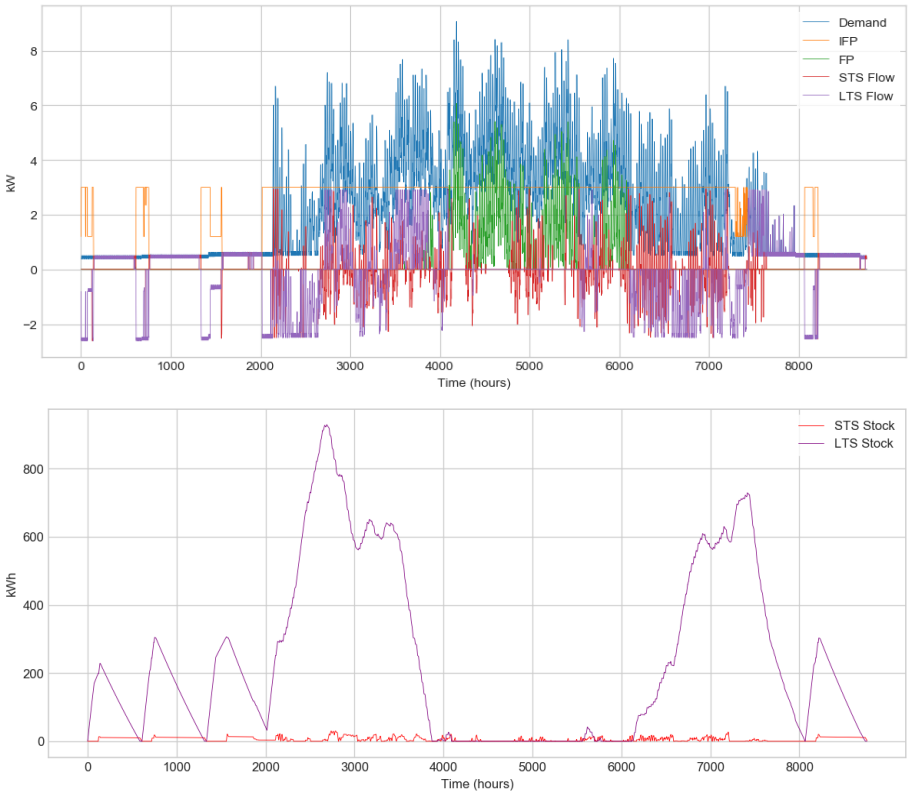

Figure 12: Results for the RP-CF-SetUp model.

The myopic approach shows nearly no use of the LTS. It makes the IFP cycling a lot. This is due to the fact that it does not anticipate set up costs after 48 hours.

In the a posteriori optimization solution, the IFP is started up only few times during the summer to limit set-up costs. The storage is filled up to 650 units before the heating season.

The M-LP model makes the IFP cycle as much as the myopic approach before the heating season (the same phenomena occurs with $H2$ and HM). It makes use of the LTS (which is not the case with HM) but stores more than the a posteriori optimization. This is due to the fact that it does not anticipate the destocking flow capacity of the LTS and the demand flows lower than the IFP capacity. Hence the stored quantity is held longer than expected which implies more losses.

The M-LP-SetUp model makes longer cycles with the IFP (the same phenomena occurs with $H2$ and HM). It stands far from the cycling strategy of the a posteriori optimization because the minimum capacity of the IFP is not considered on the LH. Hence, future costs are under-estimated. The inclusion of set-up costs also add a phase where the IFP is used at minimum capacity (before the heating season).

The RP-CF model also makes the IFP cycle a lot (to a lesser extent that the myopic or the M-LP models). It also stores less units before the heating season, which is an improvement compared to the M-LP model.

Finally, the RP-CF-SetUp model has an efficient cycling strategy on summer which is comparable to the a posteriori optimization. The model also stores units at the end of the heating season, contrarily to the a posteriori optimization. One explanation is that the approximation with RPs led to an overestimation of future costs on these periods.

4.4. Discussion and recommendations

Solutions quality. All approaches bring savings compared to the myopic benchmark approach (see Figure 6). In most cases, RP-CF approaches yield better

solutions than M-LP approaches. The difference is more significant with $H1$. These savings are also significant compared to the upper and lower bounds obtained by the a posteriori optimization. The difference with the a posteriori optimization is due to the model approximations and to the aggregation of future data.

Computation times. Table 2 shows the computation times for the different approaches (Appendix B provides further information on the convergence of the a posteriori optimization). The inclusion of a long-term horizon with the M-LP and M-LP-SetUp approaches does not significantly impact computation times. Computation times with HM increased because the relative gap was not adapted to the horizon length (the objective is optimized down to the euro for horizons $H1$ and $H2$ while it is optimized down to the tenths of euro on the HM horizon which is over-qualitative). On the other hand, computation times are three times higher for the RP-CF models on $H1$. It further increases when moving to $H2$ and HM horizons. The RP-CF-SetUp model with $H2$ needed a second year of simulation to converge: the first year ended with a higher storage level than what it started with. Regarding the CFs building computation times, they can easily be reduced by using binary search techniques or parallel computations for instance. Computation times are relatively high for horizons $H2$ and HM because CFs are computed for every days and weeks of the year, while $H1$ only requires CFs for every period of 4 weeks.

What modelling aspects to include in the long-term model. Long-term models that include set-up costs give better savings. This is due to the high set-up costs: there is an interest in setting up the IFP for longer than the SH. Further applications should include decisions that have a potential long-term impact in the long-term model. Concerning the M-LP models, the problem formulation to use as a long-term approximation can be case dependent. In this case, inclusion of the IFP minimal capacity was not fruitful for instance. It led to an overestimation of future costs and units were stored for no use. A formulation that under-estimates future costs will at least perform better than the myopic

approach. This is true for M-LP models on this case study because oscillations of the system are costly.

Choice of planning horizons. Concerning M-LP approaches, the longer and the more detailed the planning horizon the better the results. This is not true for the RP-CF model which yields a better solution with $H1$. This can be explained because the continuity between the IFP discrete states is kept between SH and LH but it is lost after the first time step of LH. Hence, the RP-CF-SetUp model benefits from the large time steps of $H1$. As a consequence, the choice of the planning horizon can depend on the approach used.

5. Sensitivity analysis

A sensitivity analysis for models RP-CF-SetUp and M-LP-SetUp is performed here. The same LH is kept in both cases. Hence, $H1$ is used because it led to significantly better results with the RP-CF-SetUp model. The objective is to test the robustness of the two best approaches on similar horizons. Both models are tested with different assumptions on the data used in Section 4, and on the quality of the demand forecast.

5.1. Sensitivity on the data

First, both models on different data sets are tested. Two data modifications are crossed:

- A change in the FP costs: 44.4, 55.6, 66.8 and 78.0 €/unit are tested. A cost of 66.8 was used in Section 4 and a cost of 44.4 corresponds to the case where no CO2 emission penalties are considered (see Appendix D for details).
- A change in the profiles used for the demand, which corresponds to different meteorological scenarios. Three demand profiles A, B and C are considered (details are provided in Appendix C). Profile A was used in Section 4.

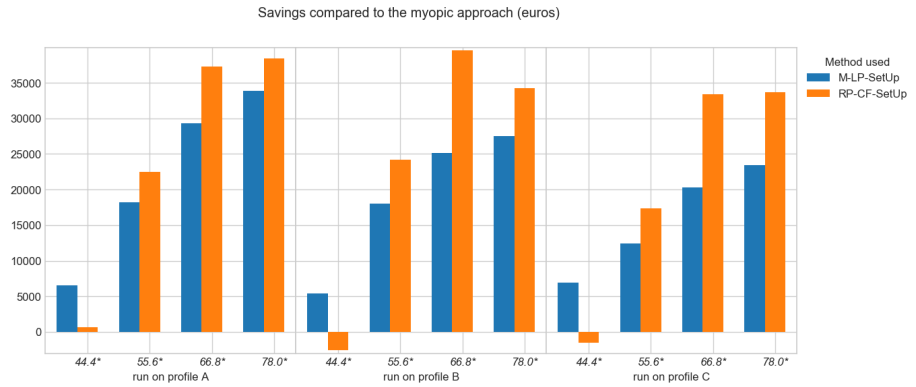

Figure 13: Savings of models RP-CF-SetUp and M-LP-SetUp on horizon $H1$, for different costs for the FP, on demand A, B and C (€). *Cost of the FP

The savings compared to the myopic model are compared for all tests, see Figure 13. Both models have steady and consistent behavior. They bring important savings on other profiles, showing reassuring stability. The exception occurs when the FP costs are low. As a matter of fact, potential saving heavily depends on the FP costs. This is because an important part of the savings comes from an efficient management of the IFP during the summer and intermediate seasons. If the FP costs are lowered, it is used during the summer instead of the IFP. In addition, the small difference between the FP and IFP costs lowers the interest in the storage of units at the beginning of the heating season. This makes the RP-CF-SetUp model slightly less performing than the myopic model: units are stored but losses exceed the savings over the FP use (see Figure 14). This is due to an over-estimation of future costs which can come from the data aggregation with RPs.

Figure 14: Solution of the RP-CF-SetUp model in case where the FP cost is 44.4 euros and the demand profile B is considered.

5.2. Sensitivity on the quality of forecasts

Up to now, the same profiles for the demand were used for both short-term and long-term horizons. The only biases came from the models used and data aggregation method (*i.e.* means and RPs). Now, results when different demand profiles are considered over the long-term horizon are compared (*i.e.* if forecasts are inexact after 48 hours).

This is done through two test procedures. In the first procedure, the planned meteorological profile after 48 hours differs from the realized profile. However, monthly total demands are constant between the planned and the realized profile. This way, intra-month forecast errors are modeled. In the second procedure, extra-month forecast errors are considered.

5.2.1. Sensitivity on the forecast meteorological profile: intra-month forecast errors

In this section, tests are run with profile A, B or C as effective demands (i.e. profiles used over SH) and with profile A, B, C or the mean on the three profiles as forecast demands (*i.e.* profiles used over LH). Hence, the demand is still perfectly known on SH, but not on LH.

The savings (cost difference with the myopic model) of different experiences are compared. Results are shown in Figure 15 for models RP-CF-SetUp and M-LP-SetUp.

A first observation is that savings are still significant and that the model RP-CF-SetUp outperforms the M-LP-SetUp model in all cases. Both approaches show relatively robust results with respect to the demand profile used on LH. As mentioned earlier, potential savings differ from one profile to another. Interestingly, the best results are not necessarily obtained when the same data is used over both SH and LH, and the effective demand seems to be the core element (savings are bigger for A and B, smaller for C): the models do not seem to overfit the forecast data.

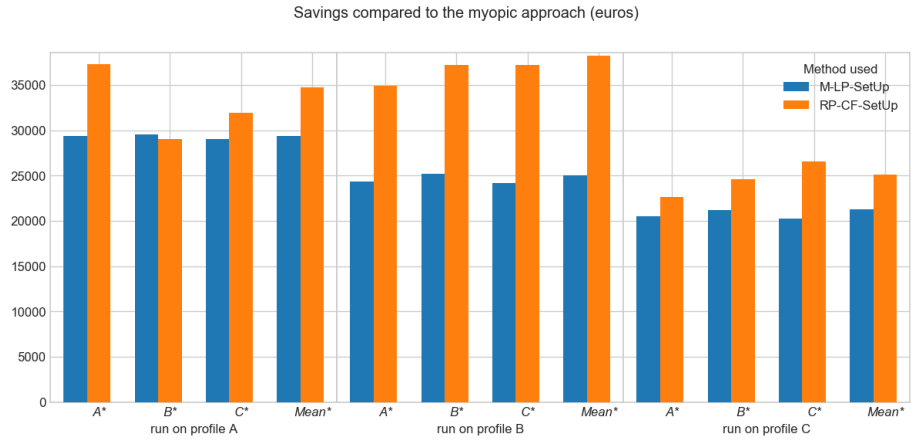

Figure 15: Savings obtained with models M-LP-SetUp and RP-CF-SetUp, on horizon H1, for different demand profiles run and planned (€). *Profile use as forecasted demand after 48 hours.

5.2.2. Sensitivity on the forecasted meteorological profile: extra-month forecast errors

Data sets A, B and C are built from different meteorological scenarios. However, the building method supposes constant monthly total demands for all data series. In order to test our models in the case of forecast errors on total monthly demands, a second test procedure is applied. A monthly forecast error is introduced: the profile used over LH corresponds to the effective profile used over SH increased or decreased by a given percentage. The demand is still perfectly known over SH, but not over LH. Three cases are tested:

- The hourly demand is always overestimated by a given percentage ($+X\%$)
- The hourly demand is always underestimated by a given percentage ($-X\%$)
- The demand is overestimated or underestimated depending on months ($\pm X\%$; the pattern used is given in Appendix C).

The savings (cost difference with the myopic model) of the different experiences are compared on Figure 16. All tests are performed with profile A.

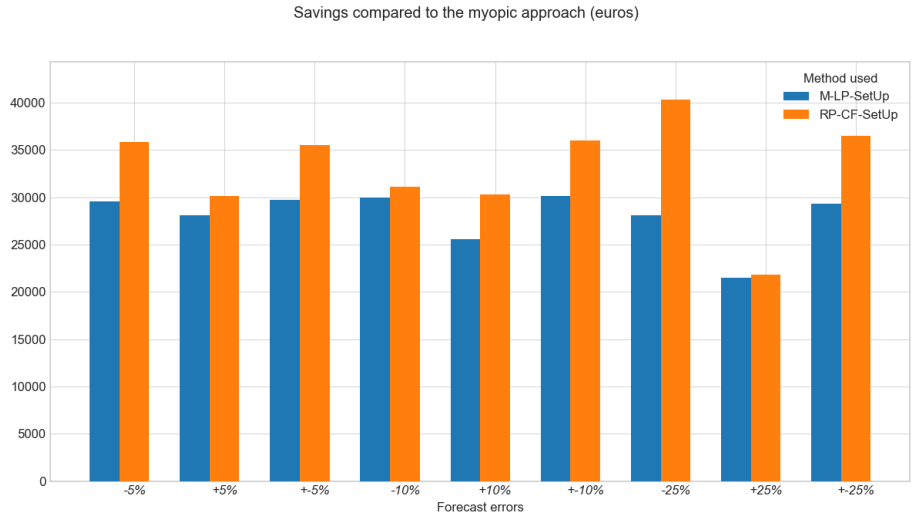

Figure 16: Savings obtained for methods RP-CF-SetUp and M-LP-SetUp on horizon H1, for different errors on the forecasted demand (€).

Similarly to Section 5.2.1, savings are still significant and the RP-CF-SetUp model remains more effective. Both models show satisfying robustness and the downgrade remains very limited as errors increase. The worst cases are when the demand is overestimated: this worsen the tendency of both model to store too many units before the heating season.

5.3. Conclusion of the sensitivity analysis

The sensitivity tests show that both models bring similar significant savings with different meteorological profiles. Modifying the cost of the FP induces significant changes in the solutions costs but this is not surprising: this parameter is decisive. Hence, this does not question the models relevancy but informs us on the models behaviour for different data. In this case, the difference in the solution costs between models is lowered. Additionally, the sensitivity analysis on the quality of forecasts suggests that both models yield robust solutions, even with forecast errors. This quality is precious for planning models.

6. Conclusion and perspectives

Rolling horizon optimization methods are relevant to recurrent and dynamic problems where immediate decisions must be made while they depend on upcoming ones. These decisions can rely on forecasts that can be updated at each optimization step. This paper focuses on problems where detailed short-term decisions can have an impact on very distant ones and vice-versa. This highly increases the temporal dimension of the problem that has to be solved at each step. Hence, there is a need to adapt the way long-term decisions are modeled.

For this purpose, two new approaches that include long-term decisions while keeping a detailed short-term formulation and a reasonable problem size are proposed. Both approaches rely on aggregated time steps that are adaptive to the forecasts accuracy. In the first approach, long-term data and decisions are aggregated as means, with a simplified long-term model. In the second approach, long-term decisions are accounted by cost functions. Cost functions are estimated with representative periods of future data and with the original detailed model. The two approaches are described and evaluated on a case study describing a heat production problem. Different versions of both approaches are tested and compared with benchmark models. Finally, a sensitivity analysis on the data is performed.

Both models show promising performances and can be implemented to include long-term decisions in rolling horizon approaches. The first one is easy to implement and has low and stable computation times. An advantage is that the continuity between state variables is kept over the whole planning horizon. A drawback is that it can miss optimal solutions depending on the problem structure and data. The second model is more costly to apply: it requires some parameterizations and pre-computations. The continuity between the storage states is kept over the whole planning horizon while the continuity between the inflexible production discrete states is only kept until a certain point. However, this can be sufficient and the second model still outperforms the first one with limited computation times. Both show robust performances under sensitivity

analysis, but their potential generalisation to further case studies should be questioned. For this purpose, a study of the generalisation aptitude on typical cases is provided as Supplementary Material with the online version of this article. Finally, all decisions with a long-term impact should be included in the long-term model, which can be more or less challenging depending on the approach. For instance, possible computation burdens for the second approach can be anticipated if several long-term decisions have to be included, as this would lead to multi-variable costs functions.

Future work will include the application of the approaches to other case studies, for both optimization and simulation purposes. Other slicing for the planning horizon can be tested and the method to build cost functions can be improved to reduce computation times. Finally, the second method offers the possibility to learn on future operational costs on the basis of more accurate models. For instance, if an optimization model gives instructions to a physical simulator or a real system, the feedback can be included in the cost functions.

Appendix A. Computation of cost functions

In this Appendix, the method for pre-computing cost functions (CFs) is detailed for the horizon $H1$ (see Figure 4), for a fixed horizon of 24 hours and for the data of Table 2. As mentioned earlier, CFs are defined for all periods t and all dates τ. However the number of CFs is only determined by the fixed horizon size. Here, as the fixed horizon is one day, 365 functions will be needed to simulate a year.

These functions are estimated by solving the original problem over one or several representative period(s) (RP) of the period t, for all t and for various values of δ.

The Python script used to build the cost functions is available at [30]. The script modifies the input files and calls the PERSEE software (see Section 4).

Computation steps for CFs for $H1$:

1. The hourly data of the year is subdivided into 13 periods of 4 weeks. Each period of 4 weeks is approximated by one or more RPs of chosen size, based on the method proposed by [31]. If several RPs are used, the method proposed by [31] provides weights for each RP such that the weighted sum of all RP days equals the number of days in the original period. The periods selected are those that minimise the difference between the duration curves of the original data and the one of the (weighted) RPs (a duration curve represents the given curve sorted by decreasing ordinate values). An example is given for two RPs of 2 days for a given period (Figure A.17, Figure A.18, Figure A.19 and Figure A.20).
2. Bounds over the minimal and maximal stored quantity (Δ_t) are set as well as the number of points to be evaluated. This defines the accuracy of the CF approximation.
3. For each period and for each point defined at Step 3, the CF $c_{\tau,t}(\Delta_t)$ is evaluated by solving the original MILP formulation of the problem (given in Section 5.2.1) over the corresponding RP(s) defined at Step 2. Costs are extrapolated so that they correspond to the size of the original period (4

weeks). This is done by multiplying the RPs costs by their weight obtained at Step 2. For instance, if 4 weeks are approximated by a 2-day RP, results are multiplied by 14. In the case of (Figure A.17, Figure A.18 and Figure A.19, the 4 weeks are approximated by two 2-day RPs with different coefficients (their sum is equal to 14). The 13 CFs obtained correspond to a single τ (see Figure A.21). Obtained functions are convex. Hence they are modelled as piecewise linear functions by the mean of Special Order Set (SOS) variables [32].

4. In order to obtain all 365 CFs, the 13 CFs obtained at Step 4 are extrapolated by weighted sums.

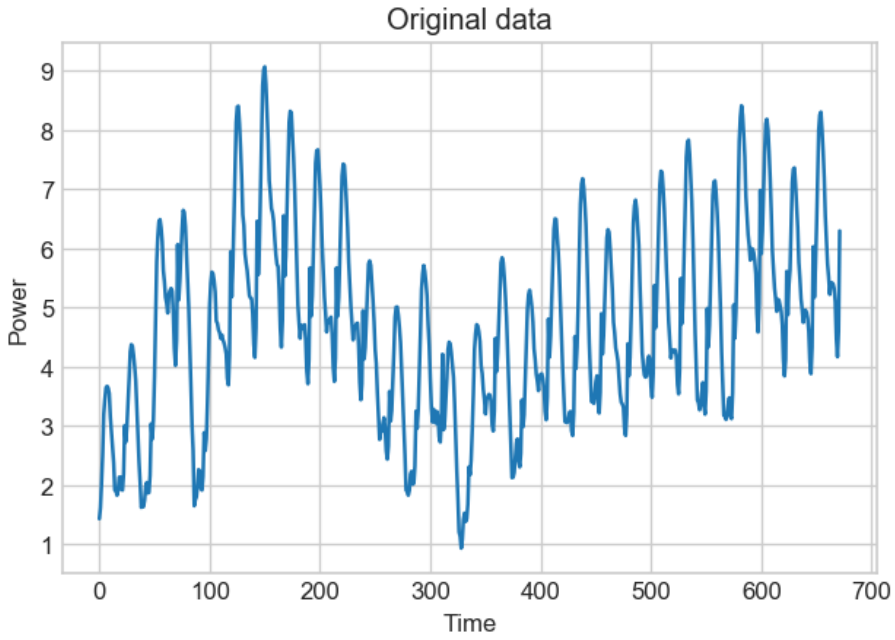

Figure A.17: Example of original data for a period of 4 weeks

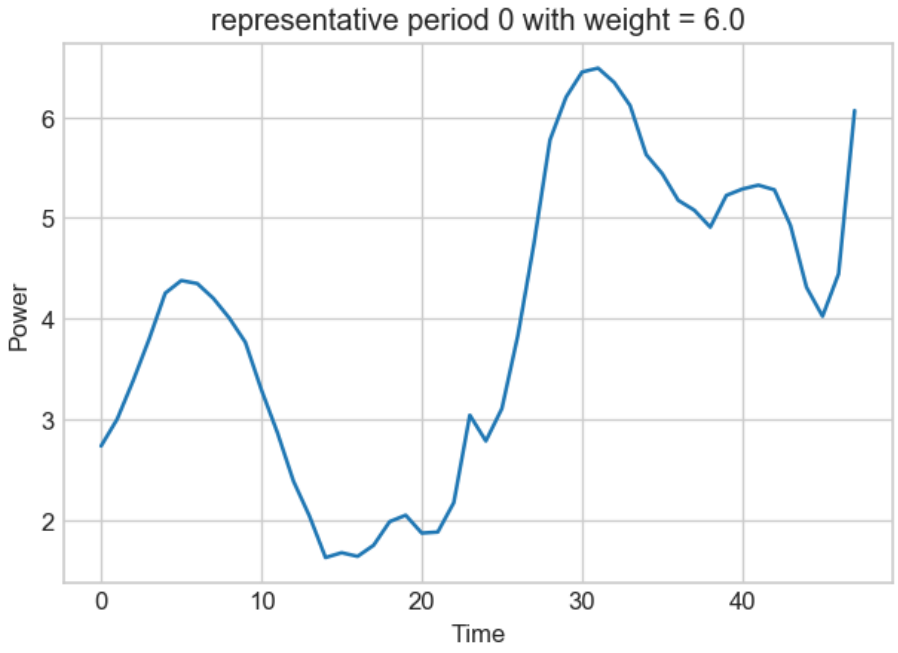

Figure A.18: First RP of 2 days for the original data.

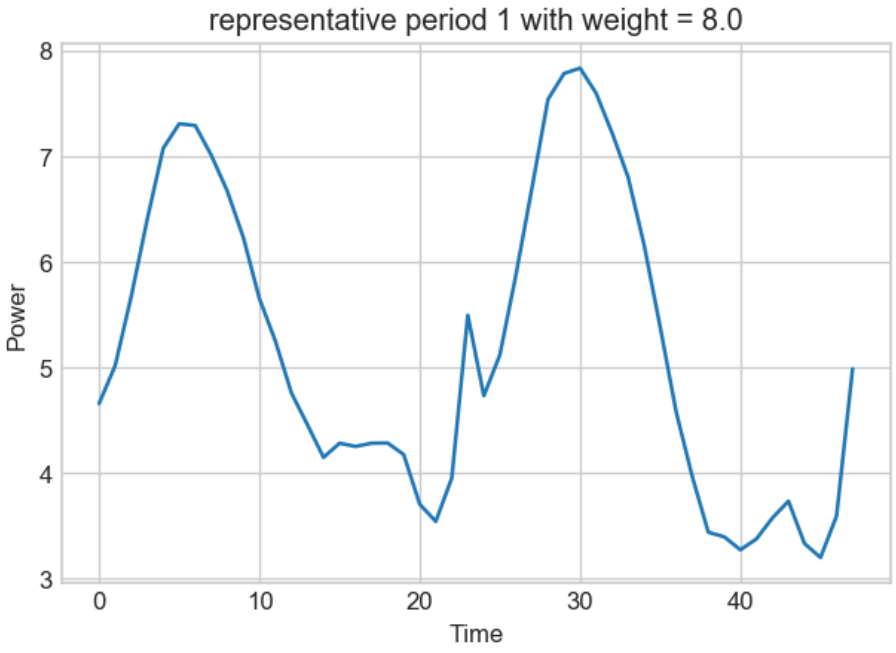

Figure A.19: Second RP of 2 days for the original data.

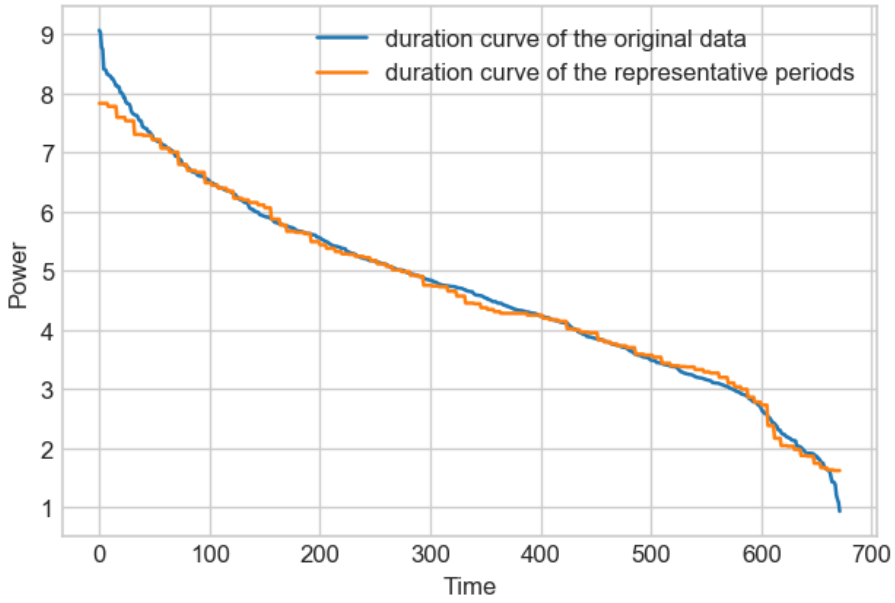

Figure A.20: Corresponding duration curves for both original and RPs, the method minimises the difference between both curves.

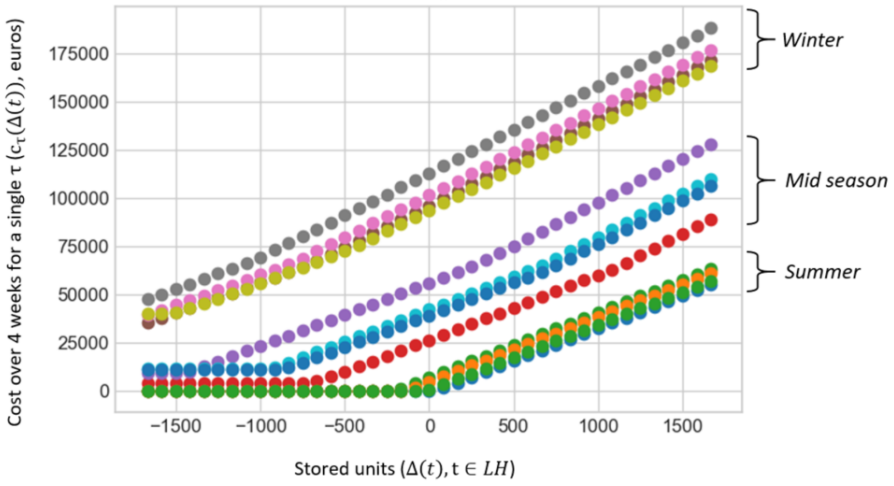

Figure A.21: Computed cost functions

Appendix B. Convergence of the a posteriori optimization

Table B.3 provides extra information on the convergence speed of the a posteriori optimization. Computations were stopped after 40 hours.

Table B.3: Lower, upper bounds and relative gap of the a posteriori optimization in function of the running time.

Time (seconds)	Lower bound	Upper bound	Gap (%)
0	800264	1278809	37.42
60	803667	1278809	37.16
90	803667	850715	5.53
91	803667	828029	2.94
95	803667	817584	1.70
1000	804117	814578	1.28
40 hours	806435	814863	1.03

Appendix C. Demand profiles

The demand profiles correspond to the heat consumption of 5000 inhabitants. It is estimated by the method used in [15] with 3 different meteorological profiles: A, B and C. The monthly mean demands are the same for all profiles. Figure C.22 shows the hourly heat demand profiles over a year, starting from July. At the hottest periods of the year, the heat demand only corresponds to hot water for sanitary use. This is supposed independent from the meteorological profile, hence, all profiles are similar on these periods. Profile A is used in Section 4, all are considered in Section 5.

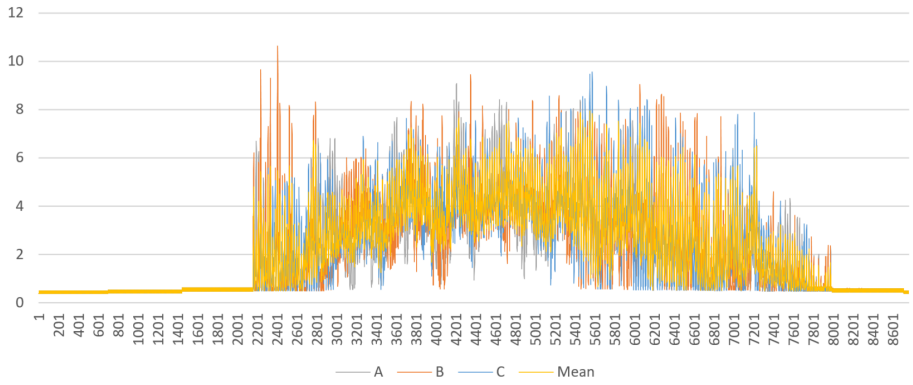

Figure C.22: Demand profiles

Table C.4 shows the arbitrary pattern which is used to artificially overestimate or underestimate ($\pm X\%$) the future demand, depending on the month, as explained in Section 5.2.2.

Table C.4: Pattern of over (+) or under (−) estimation for the error term of the forecast demand.

Jan	Feb	Mar	Apr	May	Jun	Jul	Aug	Sep	Oct	Nov	Dec
+	−	+	+	−	+	−	−	+	+	−	−

Appendix D. Production costs

Flexible production cost

The production cost of the FP is computed from the equation $C^F = (C^{CH4} + C^{CO2} * CO2^{CH4}_{content})/LHV^{CH4}/\eta^F$, where C^{CH4} is the gas cost (0.4 $euro/kg$), C^{CO2} is the CO2 emissions cost (0.06 $euro/kg$ in Section 4), $CO2^{CH4}_{content}$ is the gas CO2 content (3.36 kg^{CO2}/kg^{CH4}), LHV^{CH4} is the gas low heat value (0.01 MWh/kg) and η^F is the efficiency of the FP (0.9).

In Section 5, the different values tested for the FP production cost correspond to the respective CO2 emissions costs of 0, 0.03, 0.06 and 0.09 $euro/kg$.

Inflexible production variable cost

The variable cost of the IFP is computed from the equation $C^F = C^{biomass}/LHV^{biomass}/\eta^I$, where $C^{biomass}$ is the biomass cost (0.12 $euro/kg$), $LHV^{biomass}$ is the biomass low heat value (0.004 MWh/kg) and η^I is the efficiency of the IFP (0.9). CO2 emissions from the biomass life-cycle are supposed to be null.

References

[1] S. Chand, V. N. Hsu, S. Sethi, Forecast, solution, and rolling horizons in operations management problems: A classified bibliography, Manufacturing & Service Operations Management 4 (1) (2002) 25–43.

[2] F. Sahin, A. Narayanan, E. P. Robinson, Rolling horizon planning in supply chains: review, implications and directions for future research, International Journal of Production Research 51 (18) (2013) 5413–5436. doi:10.1080/00207543.2013.775523.

[3] J. F. Marquant, R. Evins, J. Carmeliet, Reducing computation time with a rolling horizon approach applied to a MILP formulation of multiple urban energy hub system, Procedia Computer Science 51 (2015) 2137–2146. doi:10.1016/j.procs.2015.05.486.

[4] T. Ommen, W. B. Markussen, B. Elmegaard, Comparison of linear, mixed integer and non-linear programming methods in energy system dispatch modelling, Energy 74 (2014) 109–118. doi:10.1016/j.energy.2014.04.023.

[5] M. Carrion, J. Arroyo, A computationally efficient mixed-integer linear formulation for the thermal unit commitment problem, IEEE Transactions on Power Systems 21 (3) (2006) 1371–1378. doi:10.1109/TPWRS.2006.876672.

[6] L. Giraud, M. Merabet, R. Bavière, M. Vallée, Optimal control of district heating systems using dynamic simulation and mixed integer linear programming, in: 12th International Modelica Conference., 2018. doi:10.3384/ecp17132141.

[7] M. Costley, M. J. Feizollahi, S. Ahmed, S. Grijalva, A rolling-horizon unit commitment framework with flexible periodicity, International Journal of Electrical Power & Energy Systems 90 (2017) 280–291. doi:10.1016/j.ijepes.2017.01.026.

[8] I. Blanco, D. Guericke, A. Andersen, H. Madsen, Operational planning and bidding for district heating systems with uncertain renewable energy production, Energies 11 (12) (2018) 3310. doi:10.3390/en11123310.

[9] J. Silvente, G. M. Kopanos, E. N. Pistikopoulos, A. Espuña, A rolling horizon optimization framework for the simultaneous energy supply and demand planning in microgrids, Applied Energy 155 (2015) 485–501. doi:10.1016/j.apenergy.2015.05.090.

[10] A. Saint-Pierre, P. Mancarella, Active distribution system management: A dual-horizon scheduling framework for DSO/TSO interface under uncertainty, IEEE Transactions on Smart Grid 8 (5) (2017) 2186–2197. doi:10.1109/TSG.2016.2518084.

[11] T. Schulze, K. McKinnon, The value of stochastic programming in day-ahead and intra-day generation unit commitment, Energy 101 (2016) 592–605. doi:10.1016/j.energy.2016.01.090.

[12] M. Zhou, B. Wang, J. Watada, Deep learning-based rolling horizon unit commitment under hybrid uncertainties, Energy 186 (2019) 115843. doi:10.1016/j.energy.2019.07.173.

[13] M. Wirtz, M. Hahn, T. Schreiber, D. Müller, Design optimization of multi-energy systems using mixed-integer linear programming: Which model complexity and level of detail is sufficient?, Energy Conversion and Management 240 (2021) 114249. doi:10.1016/j.enconman.2021.114249.

[14] M. Hermans, K. Bruninx, E. Delarue, Impact of CCGT start-up flexibility and cycling costs toward renewables integration, IEEE Transactions on Sustainable Energy 9 (3) (2018) 1468–1476.

[15] N. Lamaison, S. Collette, M. Vallée, R. Bavière, Storage influence in a combined biomass and power-to-heat district heating production plant, Energy 186 (2019) 115714. doi:10.1016/j.energy.2019.07.044.

[16] J. Bai, W. Wei, L. Chen, S. Mei, Rolling-horizon dispatch of advanced adiabatic compressed air energy storage based energy hub via data-driven stochastic dynamic programming, Energy Conversion and Management 243 (2021) 114322. doi:10.1016/j.enconman.2021.114322.

[17] G. Goeijen, G. Smit, J. Hurink, Improving an integer linear programming model of an ecovat buffer by adding long-term planning, Energies 10 (12) (2017) 2039. doi:10.3390/en10122039.

[18] A. Helseth, B. Mo, A. Lote Henden, G. Warland, Detailed long-term hydro-thermal scheduling for expansion planning in the nordic power system, IET Generation, Transmission & Distribution 12 (2) (2018) 441–447. doi:10.1049/iet-gtd.2017.0903.

[19] J. Shin, J. H. Lee, M. J. Realff, Operational planning and optimal sizing of microgrid considering multi-scale wind uncertainty, Applied Energy 195 (2017) 616–633. doi:10.1016/j.apenergy.2017.03.081.

[20] D. Y. Shu, N. Baumgärtner, M. Dahmen, U. Bau, A. Bardow, Optimal operation of energy systems with long-term constraints by time-series aggregation in receding horizon optimization, ECOS 2019 - The 32nd International Conference On Efficiency, Cost, Optimization, Simulation And Environmental Impact Of Energy Systems (2019) 1971–1980.

[21] A. Bischi, L. Taccari, E. Martelli, E. Amaldi, G. Manzolini, P. Silva, S. Campanari, E. Macchi, A rolling-horizon optimization algorithm for the long term operational scheduling of cogeneration systems, Energy 184 (2019) 73–90. doi:10.1016/j.energy.2017.12.022.

[22] S. Upadhya, W. J.M., A dispatch optimization model for hybrid renewable and battery systems incorporating a battery degradation model, ASME 2021 15th International Conference on Energy Sustainability collocated with the ASME 2021 Heat Transfer Summer Conferencedoi:10.1115/ES2021-63425.

[23] M. J. Reno, J. A. Azzolini, B. Mather, Variable time-step implementation for rapid quasi-static time-series (QSTS) simulations of distributed PV, in: 2018 IEEE 7th World Conference on Photovoltaic Energy Conversion (WCPEC) (A Joint Conference of 45th IEEE PVSC, 28th PVSEC 34th EU PVSEC), 2018, pp. 1626–1631. doi:10.1109/PVSC.2018.8547744.

[24] G. Savvidis, K. Hufendiek, Variable time resolution in LP electricity market and investment models, 15th International Conference on the European Energy Market (EEM). (2018) 1–5doi:10.1109/EEM.2018.8470014.

[25] A. Federgruen, M. Tzur, Minimal forecast horizons and a new planning procedure for the general dynamic lot sizing model: Nervousness revisited, Operations Research 42 (3) (1994) 456–468. doi:10.1287/opre.42.3.456.

[26] B. Guinot, B. Champel, F. Montignac, E. Lemaire, D. Vannucci, S. Sailler, Y. Bultel, Techno-economic study of a pv-hydrogen-battery hybrid system for off-grid power supply: Impact of performances' ageing on optimal system sizing and competitiveness, International Journal of Hydrogen Energy 40 (2014) 623–632. doi:10.1016/j.ijhydene.2014.11.007.

[27] M. Vallée, V. Seguin, V. Vuillerme, N. Lamaison, M. Descamps, R. Bavière, An efficient co-simulation and control approach to tackle complex multi-domain energetic systems: concepts and applications of the pegase platform, ECOS 2019 - THE 32ND INTERNATIONAL CONFERENCE ON EFFICIENCY, COST, OPTIMIZATION, SIMULATION AND ENVIRONMENTAL IMPACT OF ENERGY SYSTEMS 40 (2019) 623–632. URL https://www.researchgate.net/publication/335396048_An_efficient_co-simulation_and_control_approach_to_tackle_complex_multi-domain_energetic_systems_concepts_and_applications_of_the_PEGASE_platform

[28] E. Cuisinier, C. Bourasseau, A. Ruby, P. Lemaire, B. Penz, Techno-economic planning of local energy systems through optimization models:

a survey of current methods, International Journal of Energy Research 45 (2020) 4888–4931. doi:10.1002/er.6208.

[29] CPLEX documentation.
URL https://www.ibm.com/support/knowledgecenter/fr/SSSA5P_12.7.1/ilog.odms.studio.help/Optimization_Studio/topics/COS_home.html

[30] E. Cuisinier, Cost functions script.
URL https://github.com/EtienneCuisinier/costFunctions

[31] K. Poncelet, H. Hoschle, E. Delarue, A. Virag, W. Drhaeseleer, Selecting representative days for capturing the implications of integrating intermittent renewables in generation expansion planning problems, IEEE Transactions on Power Systems 32 (3) (2017) 1936–1948. doi:10.1109/TPWRS.2016.2596803.

[32] CPLEX documentation-SOS variables.
URL https://www.ibm.com/support/knowledgecenter/SSSA5P_12.10.0/ilog.odms.cplex.help/CPLEX/UsrMan/topics/discr_optim/sos/02_SOS_defn.html

Declaration of interests: none.